This article was downloaded by:
On: *16 January 2011*
Access details: *Access Details: Free Access*
Publisher *Taylor & Francis*
Informa Ltd Registered in England and Wales Registered Number: 1072954 Registered office: Mortimer House, 37-41 Mortimer Street, London W1T 3JH, UK

Journal of Energetic Materials
Publication details, including instructions for authors and subscription information:
http://www.informaworld.com/smpp/title~content=t713770432

A "Nanovision" of the Physiochemical Phenomena Occurring in Nanoparticles of Aluminum

Alba L. Ramaswamy[a]; Pamela Kaste[b]
[a] ECE Department, University of Maryland at College Park, MD, USA [b] U.S. Army Research Laboratory, Aberdeen Proving Grounds, MD, USA

To cite this Article Ramaswamy, Alba L. and Kaste, Pamela(2005) 'A "Nanovision" of the Physiochemical Phenomena Occurring in Nanoparticles of Aluminum', Journal of Energetic Materials, 23: 1, 1 — 25
To link to this Article: DOI: 10.1080/07370650590920250
URL: http://dx.doi.org/10.1080/07370650590920250

PLEASE SCROLL DOWN FOR ARTICLE

Full terms and conditions of use: http://www.informaworld.com/terms-and-conditions-of-access.pdf

This article may be used for research, teaching and private study purposes. Any substantial or systematic reproduction, re-distribution, re-selling, loan or sub-licensing, systematic supply or distribution in any form to anyone is expressly forbidden.

The publisher does not give any warranty express or implied or make any representation that the contents will be complete or accurate or up to date. The accuracy of any instructions, formulae and drug doses should be independently verified with primary sources. The publisher shall not be liable for any loss, actions, claims, proceedings, demand or costs or damages whatsoever or howsoever caused arising directly or indirectly in connection with or arising out of the use of this material.

Energetic Materials, 23: 1–25, 2005
Copyright © Taylor & Francis Inc.
ISSN: 0737-0652 print
DOI: 10.1080/07370650590920250

Taylor & Francis
Taylor & Francis Group

A "Nanovision" of the Physiochemical Phenomena Occurring in Nanoparticles of Aluminum

ALBA L. RAMASWAMY

ECE Department, University of Maryland at College Park, MD, USA

PAMELA KASTE

U.S. Army Research Laboratory, Aberdeen Proving Grounds, MD, USA

Downloaded At: 13:46 16 January 2011

High-resolution transmission electron microscopy of nanoparticles of aluminum has resolved the oxide surface and aluminum lattice down to atomic level. The oxide was found to be about 2.5 nm in thickness with a part amorphous and part crystalline nature. It appears highly porous, allowing the permeation of water molecules from humidity, linkable with the aging characteristics. The aluminum crystal lattice revealed a slight compressive stress. A model of the oxidation was developed to characterize the process. Finally the presence of impurities detected in the nanoaluminum is revealed as a trigger to low-temperature (below the melting point) autocatalytic reactions.

Keywords: pyrotechnics, propellant, rocket

Address correspondence to A. Ramaswamy, ECE Department, University of Maryland at College Park, College Park, MD, 20742 USA. E-mail: alr33@cam.ac.uk

Introduction

Aluminum is the third most abundant element in weight after oxygen and silicon in the earth's crust. It is very reactive, with a high heat of combustion, and some of its reactions proceed with explosive violence. The rapid formation of a thin layer of the oxide, however, prevents the further attack by oxygen and retards chemical reactions of the aluminum as, for example, with acids. When pure aluminum is heated in dry oxygen, it reacts vigorously, forming a layer of aluminum oxide, which prevents its further attack. The property of this protective oxide allows the use of aluminum, a very light, malleable, ductile, and abundant metal in numerous applications. The thin oxide layer is considered to be nonporous, very different from iron metal, which forms a porous oxide layer of rust, readily penetrable by water, with corrosion proceeding beneath the superficial layer of the rust.

In the case of the use of aluminum in solid rocket propellants, the high reactivity of the metal is the most desired property. The oxide surface, on the other hand, although providing good aging characteristics to the fuel additive, often has been considered in the literature [1, 2] as a less than desirable property for the rapid and efficient release of heat from the metal. In fact, the order of amount of heat release per unit volume of typical potential fuel metal additives is the following: boron > beryllium > aluminum > magnesium > lithium. Table 1 gives the heat of combustion of the metals per unit volume and unit weight, together with the electronegativity on the Pauling scale (the electronegativity of an atom provides a numerical measure of the electron attraction power for the atom or element). As can be seen from the table, although other potential metal fuel additives may release more heat per unit weight or volume, aluminum is the additive of choice in propellant compositions, primarily due to its higher availability and comparatively low cost. In addition the aluminum oxide residue in the form of particles inside a rocket motor serves a very important purpose in alleviating certain combustion instabilities, by quenching the acoustic resonant oscillations forming in rocket

Downloaded At: 13:46 16 January 2011

Table 1
Properties of potential metallic fuels compared

Metal	Heat of combustion metal kJ/cm^3	Heat of combustion of metal kJ/g	Pauling electro-negativity
Boron	−142.25	−58.90	2.0
Beryllium	−124.86	−67.64	1.0
Aluminum	−83.80	−31.06	1.5
Magnesium	−43.03	−24.76	1.5
Lithium	−22.96	−43.07	1.2

Note: Table compiled from various sources [2, 3, 4].

motors, which otherwise would lead to structural damage to the motors during flight [2]

The aluminum combustion in a solid rocket propellant and the role of the oxide were studied in detail and described in the literature. In summary, experimental observations of the standard micron-sized aluminum include microscopic studies of partially burned or heated samples, visual and photographic observation of the burning, spectroscopic observations of the flame, and collection and analysis of the reaction products [1].

When the micron-sized aluminum particles are heated on a hot stage microscope, there is little response until the melting point of 660°C is reached. The thermal expansion becomes visually evident prior to the melt. When heating is continued in inert atmospheres, the oxide skin breaks open and releases the liquid aluminum, which fuses with that of the neighboring particles to form aggregates [5, 6]. In an oxidizing atmosphere healing of the cracks occurs by surface oxidation from the gases. In this case the oozing out of molten or liquid aluminum followed by aggregation takes place at higher temperatures [6]. Evidence of crack healing comes from recovered particles, which show clear expansion crack patterns in the oxide ''healed up'' by oxidation of the emerging metal [5, 6].

Most of the particle ignition occurs in the flame and takes place in 1–50 ms [7]. The metal droplet surface temperature,

Downloaded At: 13:46 16 January 2011

at the instant of ignition, is just below the melting temperature of the oxide (2040°C), and the surrounding reacting metal vapors extend in a radial flame zone around the particles about 2 to 5 particle radii in size. In practice the temperature of the metal surface in the self-sustaining combustion is in the range of 2100–2400°C, that is, below the boiling temperature of pure aluminum.

Questions were raised in the literature [1, 2] as to whether the observed agglomeration of the micron-sized aluminum on the surface of the propellant may be impeding the combustion process and slowing the burning velocity, whether combustion of the metallic particles may be incomplete in part due to the oxide coating present on the aluminum surface, and whether condensed oxide combustion products or slag formation may result in a reduction of motor efficiency. Nanoaluminum was considered as a potential solution to these questions. In this paper a detailed study of nanoaluminum at the atomic level is described. This understanding can be important both in optimizing the use of the standard aluminum and in the tailoring of nanoaluminum with improved properties for use in propellants and other applications. Finally, it can shed light on the potential use of other additive fuels leading to the more efficient and rapid release of energy for improved and cost-effective solutions in the efficient harnessing of energy from energetic materials.

Downloaded At: 13:46 16 January 2011

Observations and Results

High-Resolution Transmission Electron Microscopy

Nanoaluminum particles have been examined at a resolution of 1.6 Å using the National Center for Electron Microscopy (NCEM) Atomic Resolution Microscope (ARM). The high-voltage JEOL ARM-1000 microscope was used at an electron energy of 800 kV and a magnification of 600 K × to ensure adequate electron beam penetration of the whole (nonsectioned) nanoaluminum particles. The electron micrographs obtained from the ARM were analyzed by computer imaging and local areas of the micrographs enlarged.

Figure 1 shows the typical ''corner'' of a nanoparticle of aluminum. As can be seen from the micrograph, an oxide layer 2.5 nm in thickness is clearly visible. The aluminum crystal lattice is evident, and the separation between the atomic planes of aluminum atoms considering a face centered cubic lattice was measured from the micrographs and found to be $\sim 4.0\,\text{Å}$, which agrees with the unit cell lattice parameter for the aluminum of $4.05\,\text{Å}$, proving that the nanoparticle consists of an apparently unstrained aluminum lattice. This is in agreement

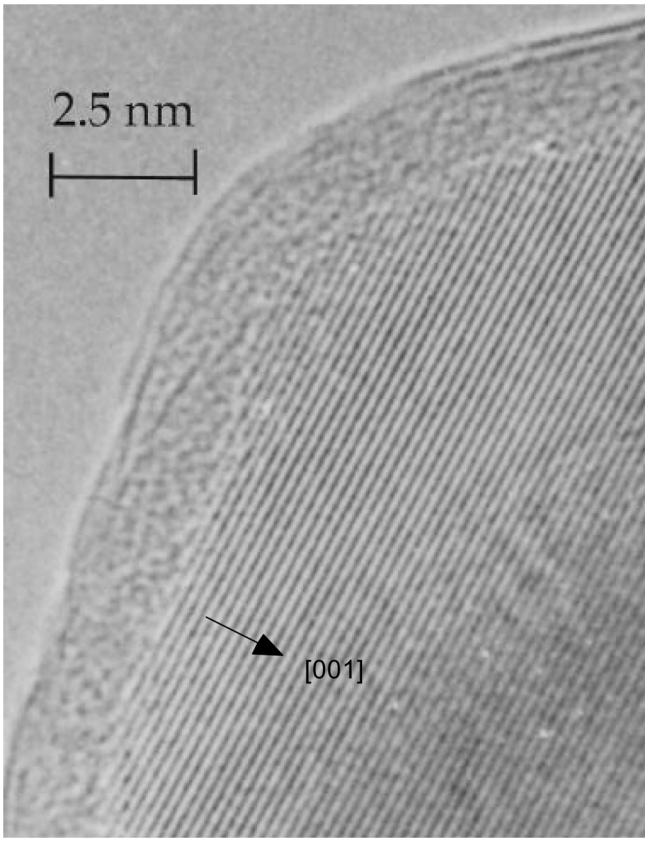

Figure 1. High-resolution electron micrograph of nano-aluminum.

Downloaded At: 13:46 16 January 2011

with X-ray diffraction measurements reported in an earlier paper [8].

The aluminum oxide surface appears to be primarily amorphous, in agreement with the X-ray data [8]. A closer examination of the micrographs indicates that some areas of the oxide are arranged in single molecular sheets, the smallest ones 10 to 20 molecules in length. In fact, chemical analysis of the nanoaluminum by Prompt Gamma Neutron Activation Analysis (PGAA), reported in an earlier paper [8], evidences a large fraction of hydroxide together with absorbed humidity or water molecules and boron impurities. Thus the outermost oxide layer gradually gets converted to hydroxide in contact with atmospheric humidity. The molecular layer on the particle surface can be seen to consist of a single crystalline layer. There is thus localized crystalline order, both on the surface of the particles and in localized areas within the oxide/hydroxide surface not detectable by X-ray diffraction.

Figure 2 shows another area from a different nanoparticle. Several crystalline molecular layers can be seen clearly to cover the oxide/hydroxide surface of the particle. The rest of the oxide is amorphous with localized crystalline order in other areas. The molecular layers appear to superimpose with some crystalline mismatch.

The crystalline mismatch in the molecular layers of the surface oxide indicates that they may tend to exfoliate readily. This is confirmed by examination of the electron micrographs, of which Figures 3 and 4 are examples.

From the PGAA measurements reported in the earlier paper [8] it was determined that the surface layer primarily consists of aluminum hydroxide, for samples where humidity has come into contact with the material. Also moisture or water molecules were found trapped within the intermolecular spacing of the hydroxide. PGAA data confirmed that the nanoaluminum had absorbed twice as much water compared with standard ''flaked'' aluminum. This shows that the oxide/hydroxide surface of the nanoaluminum particles has a highly porous structure.

As described in the introduction, cracking of the oxide shell, followed by oozing of molten aluminum from the particles,

Downloaded At: 13:46 16 January 2011

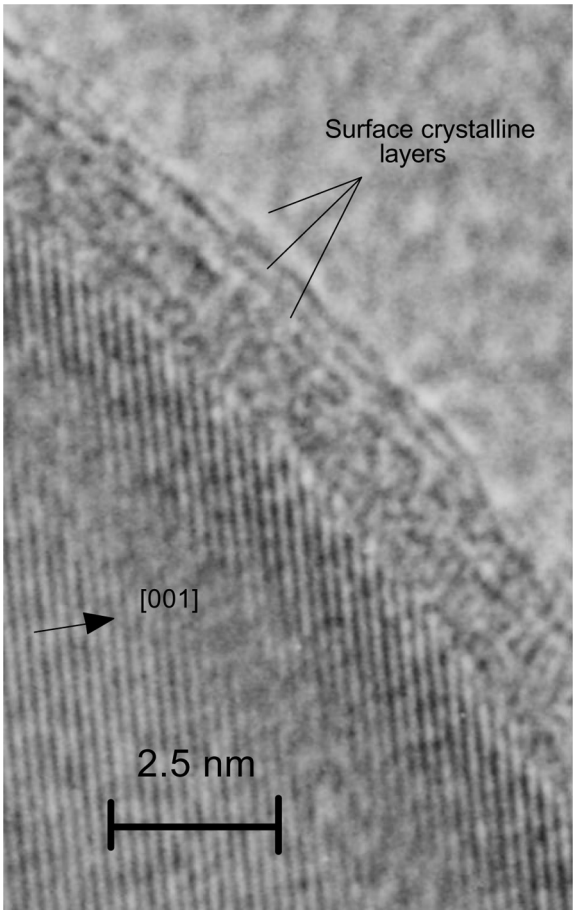

Figure 2. Nanoparticle showing layered structure in oxide/hydroxide surface and the aluminum/oxide boundary.

allows the aggregation of two or more particles of aluminum on the surface of the propellant during combustion. The nanoparticles were produced by formation of metal clusters by aggregation in a coolant gaseous atmosphere. The fusion or aggregation of two or more nanoparticles was found here to occur during the production process itself. Figure 5 shows two nanoparticles fused together with the formation of a clear grain boundary.

Downloaded At: 13:46 16 January 2011

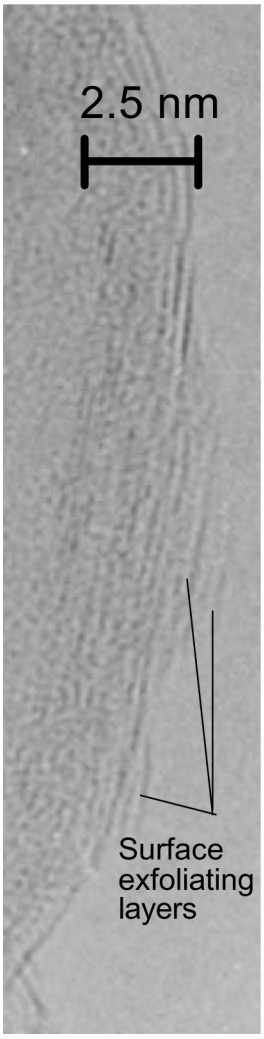

Figure 3. Exfoliation of single molecular laminar sheets from nanoaluminum coating.

With reference to crystalline impurities, PGAA analysis [8] has evidenced the presence of boron as well as hydrogen and water impurities. In fact, the nanoaluminum appears as a black powder. Crystalline boron is jet-black in color. The

Downloaded At: 13:46 16 January 2011

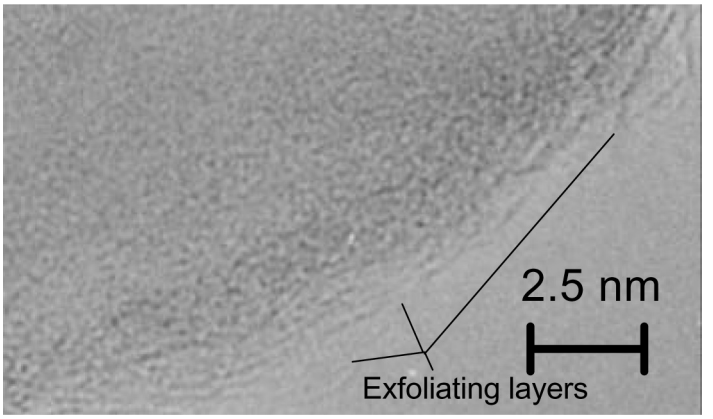

Figure 4. Exfoliation of oxide layers from surface.

Downloaded At: 13:46 16 January 2011

amount of boron impurity found indicates that the black coloration can be achieved by concentration of the boron impurity in the surface oxide/hydroxide. In fact, it was estimated that if all the boron was crystallized in one of the outermost molecular layers, it would consist of about 12% atomic boron. Furthermore iron, copper, potassium, and (nitrogen in some aluminum-ALEX samples) impurities were detected by XPS (X-ray Photoelectron Spectroscopy) [9].

The presence of light-element impurities was related to ''low''-temperature ($\sim 515^{\circ}$C) impurity-triggered autocatalytic reactions [8], formerly attributed to the phenomenon of ''structural bond release energy.'' In fact, no apparent positive strain was found stored in the nanoparticles, neither by X-ray diffraction nor from the examination of the high-resolution electron micrographs (though detailed examination of the X-ray diffraction data shows indications instead of a small amount of compressive stress, as described later). The observation of predominant lattice deformations was not found in any particle, and dislocations were extremely rare. Only one dislocation was found and imaged in one nanoparticle, as seen in Figure 6.

Aluminum hydroxide tends to occlude water molecules, easily the Al^{3+} ions clinging to electron-rich atoms. The boron ''metal'' may thus be ''held'' in the aluminum hydroxide

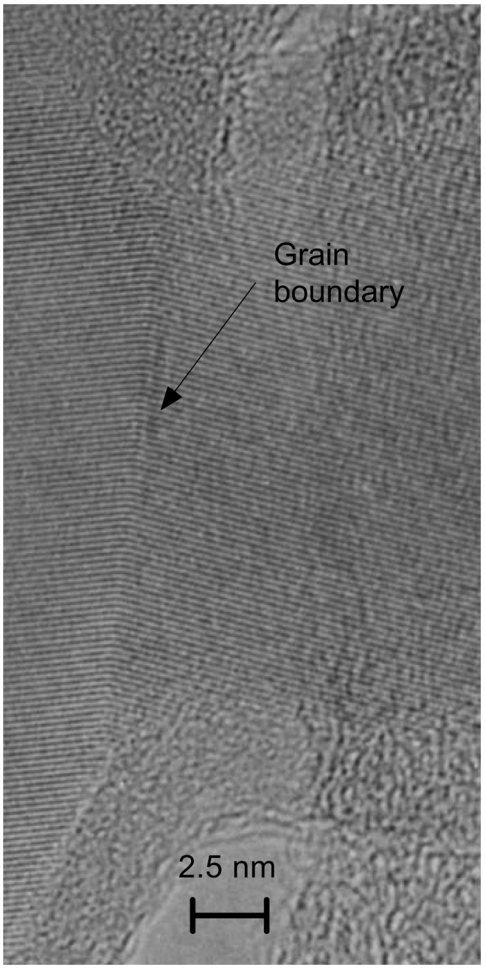

Figure 5. Grain boundary of two fused aluminum nanoparticles.

structure, giving it the black coloration. A small amount of boron oxide and possibly boric acid may also be present, by reaction of the water with boron oxide. Now, aluminum reacts with both dilute acids and alkalis producing hydrogen gas, which itself will react with oxygen, forming more water. However, when temperatures of over 100°C are reached, the

Downloaded At: 13:46 16 January 2011

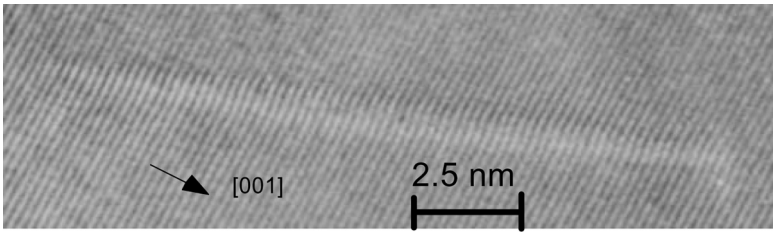

Figure 6. Dislocation in nanoparticle of aluminum.

water molecules all may have evaporated leaving boron, boron oxide, aluminum oxide, and aluminum hydroxide and iron, copper, potassium, and nitrogen impurities. Now, pure boron oxide melts at 450°C, and pure aluminum melts at 660°C. The hydroxide form present on the nanoaluminum is unstable above 450°C, and dehydrates to form alumina and water. The reactions described earlier thus can start to occur. Boron can start igniting at $\sim$830°C, in the presence of metallic impurities [2], producing larger quantities of heat as described in the Introduction. Thus the presence of the impurities may overall catalyze reactions when a temperature of 500°C is approached, and in nanoaluminum the low level of impurities has a greater weight effect or impact per nanoparticle and material as a whole, as compared with micron-sized aluminum.

Such an inference can be used constructively. For example, when one considers that nitrogen is one of the main constituent elements of explosives, the nitrogen present within the nanoaluminum potentially may be incorporated in such a way as to make the material ''part-explosive'' by triggering the appropriate physiochemical reaction. The incorporation of light-element-tailored impurities during the manufacture may provide for new improved forms of nanoaluminum by ''atomic-scale design.''

X-ray Diffraction

An X-ray diffraction scattering experiment was performed on the sample of nanoaluminum. X-ray powder diffraction (XRD)

Downloaded At: 13:46 16 January 2011

patterns were recorded using a Bruker D2 Discover X-ray Powder Diffractometer (CuKα radiation) and analyzed with an MDI software analysis system. The analyzed X-ray scattering plot obtained is shown in Figure 7 as well as reported in an earlier paper [8]. The corresponding peak positions and relative intensities for a reference sample of pure 100% aluminium are shown under the graph. These were obtained from the MDI software spectra databank. A perfect correlation can be seen. At the lower diffraction angles there is evidence of the ''beginning'' of a peak generally attributable to an amorphous or nanocrystalline material. It can be assigned most closely to nanocrystalline areas of α-aluminum oxyhydroxide (AlO(OH) $2\theta = 22$ for the most intense peak) and possibly some α-boron ($2\theta = 18$ for the most intense peak).

Table 2 gives the X-ray diffraction data for the nanoaluminum and standard flaked aluminum reported in an earlier paper [8] and resummarized with the computed strain taken as $\Delta a/a$, where a for aluminum is 4.05 Å. A detailed analysis of the X-ray diffraction data shows that the nanoaluminum particles have a small amount, on the order of 1–2%, of negative strain or compressive stress in some orientations. This might have been induced during the solidification of the oxide on the surface of the aluminum, which may have compressed the lattice by a small amount.

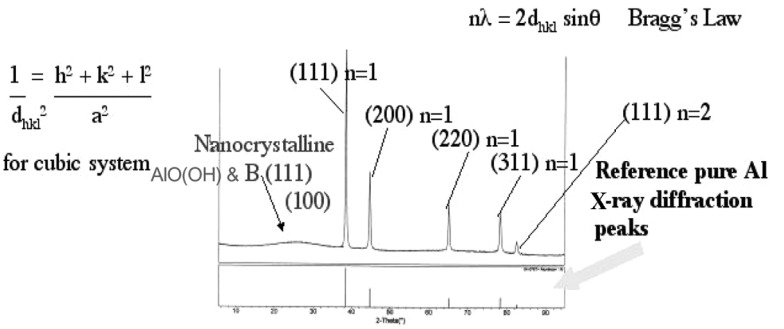

Figure 7. X-ray diffraction scattering measurements for nanoaluminum and 100% aluminum compared.

Downloaded At: 13:46 16 January 2011

Table 2
X-ray diffraction data on the standard aluminum and nanoaluminum compared

Sample	H, K, L	a (Å)	$\Delta a/a$
Al flaked	1, 1, 1	4.03 ± 0.02	0
Al nanopowder	1, 1, 1	3.96 ± 0.02	-0.017
Al flaked	2, 0, 0	4.03 ± 0.02	0
Al nanopowder	2, 0, 0	3.98 ± 0.02	-0.012
Al flaked	2, 2, 0	4.05 ± 0.02	0
Al nanopowder	2, 2, 0	4.05 ± 0.02	0
Al flaked	3, 1, 1	4.05 ± 0.02	0
Al nanopowder	3, 1, 1	4.07 ± 0.02	0

Downloaded At: 13:46 16 January 2011

Modeling of Aluminum Oxidation

Aluminum has a face-centred cubic lattice with the unit cell parameter a of 4.04958 Å. A model for the oxidation of nanoaluminum is described here where oxygen adatoms appear to be able to ''move'' through the aluminum interatomic spaces to fill the lattice until electric charge equilibrium is obtained and no further atoms can penetrate.

Figure 8 shows the face-centered cubic lattice of aluminum generated by the Crystalmaker Software [10]. The covalent atomic radius of a single oxygen atom is on the order of 0.6 Å: an oxygen molecule thus has a total length of 2.4 Å (or 4×0.6 Å). When computing the interatomic space in the fcc lattice, it is noticed that there is enough space for an oxygen molecule to enter the octahedral interstitial site of aluminum atoms on the surface in a vertical orientation, as depicted in Figures 8 and 9. In fact, when a clean aluminum metallic surface (free from oxygen and oxide) is exposed to air or oxygen, oxygen molecules will attach themselves by ordinary intermolecular (van der Waals) forces almost instantaneously. This is a physical adsorption.

The octahedral site has a diameter of 1.20 Å ($4.05 - (1.43 \times 2)$), where 1.43 Å is taken as the atomic radius

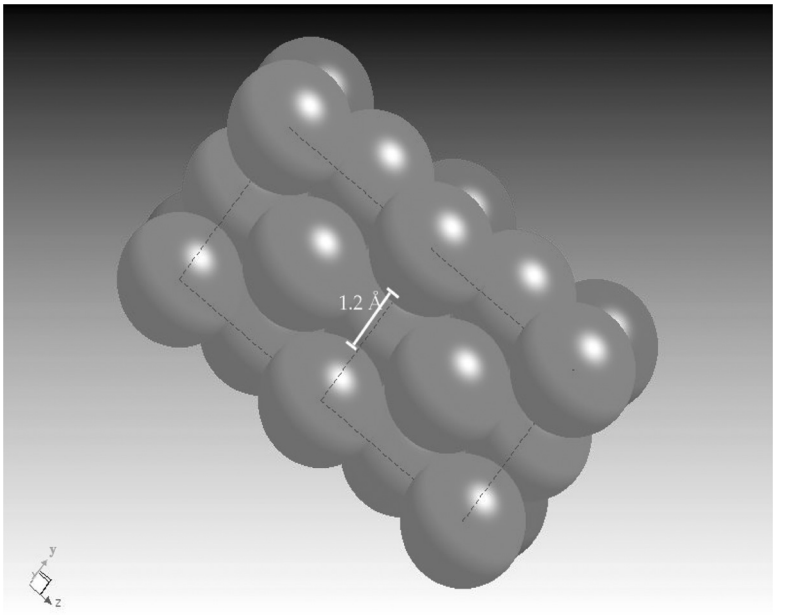

Figure 8. Face-centered cubic structure of aluminum.

Downloaded At: 13:46 16 January 2011

of an aluminum atom, which can just fit the diameter of a single oxygen atom, which is 1.20 or 2×0.6 Å. Figure 9 depicts the deposition of an oxygen molecule in the interatomic spacing of the surface aluminum atoms. Since the oxygen molecule just fits into the octahedral interstitial site of aluminum, it becomes ''clamped'' and permits the second phase to take place, namely, a combined chemisorption and dissociation of the oxygen molecule. The dissociation of the oxygen molecule produces an oxygen adatom as described in the literature [10]. This dissociation of the molecule can occur by combination and dissociation of the surface oxygen with an oxygen molecule in the gas as occurs on the surfaces of TiO_2 [11] or by the high-temperature-triggered combination of the surface aluminum atom with the oxygen molecule to form an oxygen adatom. The oxygen thus enters into combination with the metallic basis owing to electron transfer or electron sharing between oxygen and metal atoms; an oxygen molecule must attain a certain

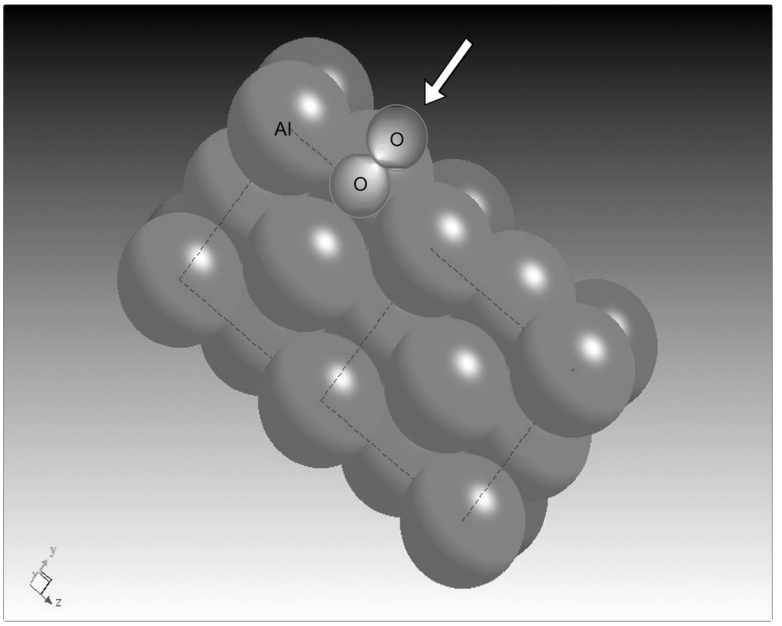

Figure 9. Deposition of oxygen molecule in octahedral interstitial site of aluminum surface.

Downloaded At: 13:46 16 January 2011

energy before this chemisorption can take place, for example, with higher temperatures. As such the covalent radii (eventually ionic) of the aluminum atoms can be taken into account and nominally applied to the model, as shown in Figure 10.

Considering the unit cell of aluminum now, the interatomic spacing between the face-centered aluminum atom and the corner atom is 0.35 Å or $((4.05^2 + 4.05^2)^{1/2} - (1.25 \times 4))/2$. This is $\sim\frac{1}{4}$ the dimension of a single ''dissociated'' oxygen atom, which is 1.20 Å. However, there is some lateral interatomic space available for the aluminum atoms to shift. The repulsion of the neighboring aluminum atoms prevents this shift unless the aluminum atoms gain energy or are in an excited state. This state can be achieved through the higher temperatures and/or by the ''combination'' of the oxygen adatom with the surrounding aluminum atoms. Thus, for example, for the oxygen atom to move into the lattice, the aluminum

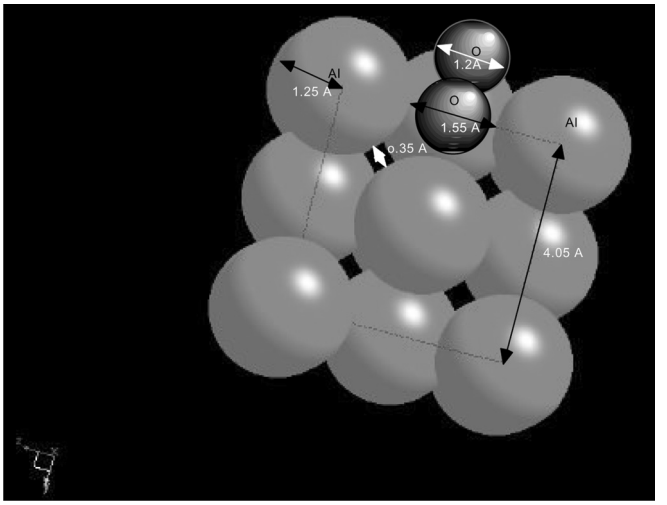

Figure 10. Insertion of oxygen molecule on aluminum surface.

Downloaded At: 13:46 16 January 2011

atoms must separate by 0.85 Å, which corresponds to a shift by each atom of 0.425 Å. Once the repulsion barrier has been overcome and the oxygen adatom slipped between the aluminum atoms, it can fit snuggly into the next octahedral interstitial site, depicted in Figure 12. When a new oxygen molecule deposits on the surface, it can "push" down the oxygen adatom. Furthermore the presence of the oxygen atom in the interatomic spacing has the effect of autocatalyzing the further oxidation, as is seen in the case of lead [12]. The autocatalysis may be due again to the excitation of the surrounding aluminum atoms by "combination" reactions with the oxygen adatoms. Thus at higher temperatures the oxide surface appears to catalyze or facilitate the further oxidation, rather than impede it. A series of "video clips" can be drawn, as shown in Figure 12 for a single unit cell, to show how the oxidation can progress to form the surface oxide.

As the oxygen atoms fill a unit cell, further oxygen molecules depositing on the surface can "push" the oxygen atoms farther down until 2.5 nm of oxide is created. This is equivalent

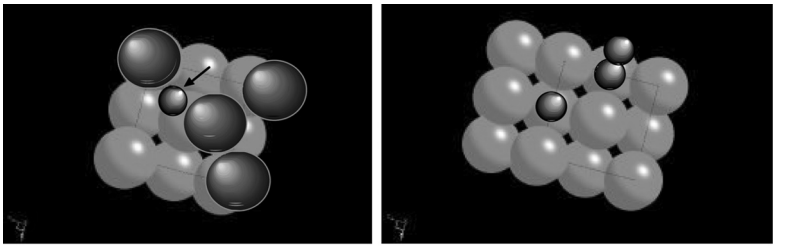

Figure 11. ''Videoclips'' of the oxidation of aluminum. (a) Oxygen adatom slips between the two aluminum atoms, which have shifted due to the ''excitation'' of the aluminum atoms shown. (b) Oxygen adatom fits in interatomic spacing, and new oxygen molecule approaches.

Downloaded At: 13:46 16 January 2011

to the ''filling'' up of 6 unit cells. No further oxidation occurs when the interatomic space is so filled up with oxygen atoms that there is no extra space for any additional ones to move into after electric charge equilibrium has been reached. From this it can be realized that single crystalline aluminum oxide is difficult to form on the surface of the aluminum, but rather an overall amorphous or part-crystalline coating is produced. Single molecular sheets, however, form prevalently on the surface of the coating. This is in agreement with the model where oxygen atoms drop into the spaces and ''fill up'' the interatomic spaces. Thus the atoms at the surface combine and separate with the oxygen atoms sequentially and have the time to settle into the final equilibrium positions. This allows for the formation of a crystalline lattice on the surface where charge equilibrium is attained.

Figure 12 shows the crystal structure of α-aluminum oxide [13], which is believed to correspond with the crystalline areas of the surface oxide. In fact, the main phase composition of the oxide, forming upon aluminum combustion in oxygen, depends on the conditions of its formation [2], the main fraction consisting of α-alumina under usual combustion conditions. In fact, during the production process of the nanoaluminum, cooling was achieved with oxygen gas, which is believed to have had

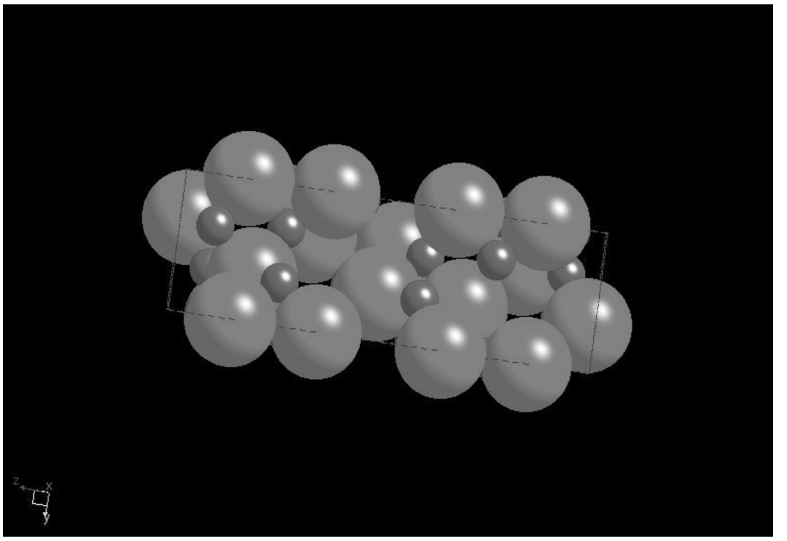

Figure 12. Unit cell of α-aluminum oxide [13].

Downloaded At: 13:46 16 January 2011

the effect of a surface combustion. The most stable phase of alumina is the α-form. Combustion in subatmospheric conditions or upon sharp cooling produces γ-alumina, which under heating to 1000 K transforms to α-alumina. The α-alumina phase is the higher density phase with a density of $3.96\,\mathrm{g/cm^3}$ compared with γ-alumina with a density of $3.42\,\mathrm{g/cm^3}$. The α-phase of alumina has a rhombohedral lattice, and γ-alumina has a cubic face-centred lattice. The rhombohedral α-form of alumina can grow into crystals with a platelet morphology, which may explain the observed surface laminar layers on the nanoaluminum, which tend to exfoliate. Both forms of alumina, if uncompressed, would occupy a greater volume than the metal destroyed in producing them. When they are first formed on the surface of a metal they will be in a state of lateral compression. The α-form will have the greater compression. Thus the formation of the more compact α-form may have transferred a small amount of its compressive stress into the aluminum of the nanoaluminum particle, since it surrounds or constrains the whole nanoparticle.

As can be seen from Figure 12, the aluminum atoms have displaced from their original equilibrium positions in the aluminum lattice to new positions in the oxide lattice, in agreement with the model. The interatomic distance between aluminum atoms on the surface corresponds with 2.654 and 3.844 Å. The oxygen atoms thus have drawn the aluminum atoms closer together from the original 4.04958 Å, in agreement with the model. It can be seen that the two aluminum atoms, which are closer, better overlay the oxygen atoms. The space between the aluminum atoms on the surface can be computed and is found to be approximately 1.254 and 2.444 Å. This is barely sufficient space for a water molecule to enter and deposit between the atoms in different orientations. By PGAA analysis it was found [8] that the nanoaluminum had absorbed a lot of water. By heating the material in a vacuum oven, the water was released, and it was found that a large amount of hydrogen still resided in the form of hydroxyl groups. This means that the nanoaluminum coating is porous, and some of the water, which deposited into the coating, reacts to form aluminum hydroxide. The surface layer is thus considered to consist of α-aluminum oxy-hydroxide [14] Al–O(OH) since there is a topotactic relationship between the two phases of α-alumina and α-aluminum oxy-hydroxide (the equivalent phases in mineralogy are termed corundum and diaspore). Thus when α-aluminum oxy-hydroxide is heated above 450°C, α-alumina is generated. The unit cell of the α-aluminum oxy-hydroxide is shown in Figure 13, together with a typical exfoliation plane along which exfoliation of molecular layers from the surface might occur.

The γ-alumina and γ-aluminum oxy-hydroxide have a more open and porous structure than the α-forms but are less stable, and according to the dehydration scheme used for measuring the hydrogen content by PGAA before and after dehydration, had the γ-form been present, there would have been greater if not total loss of hydrogen than was actually measured [8]. In fact, γ-aluminum hydroxide $Al(OH)_3$ readily reverts to γ-aluminum oxy-hydroxide Al–O(OH) at 100°C and becomes totally anhydrous, forming the γ-alumina form Al_2O_3 at 150°C [15]. Also

Downloaded At: 13:46 16 January 2011

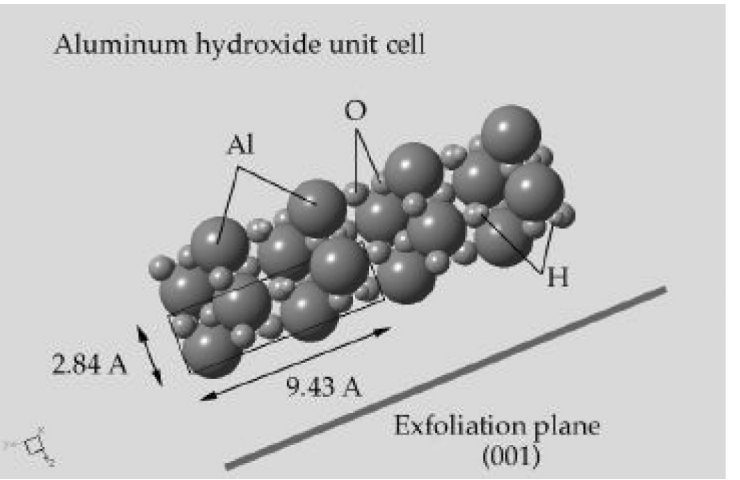

Figure 13. Unit cell of α-aluminum oxy-hydroxide: (diaspore) Al–O(OH) [14].

Downloaded At: 13:46 16 January 2011

from the X-ray diffraction data, it appears that the formation of the α-forms of alumina, with mismatched intercrystalline layers where water molecules can deposit and gradually penetrate into the structure to form α-aluminum oxy-hydroxide, is highly likely. Furthermore γ-alumina is typically white in color, and α-alumina is transparent but readily takes on the color of the impurities it contains (e.g., ruby is α-alumina with red Cr^{3+} ions, sapphire is α-alumina with blue Fe^{2+}, Fe^{3+}, and Ti^{4+}, emerald is green with V^{3+}, and similarly for amethyst and topaz, etc.) The nanoaluminum gave no evidence of a surface white coloration but had a marked black color in agreement with boron impurities in an α-alumina or α-aluminum oxy-hydroxide surface structure.

A third form of aluminum oxide is known to form as a protective layer on metals [15]. It is the one typically formed on larger sheets of aluminum metal and has a defect NaCl-type structure with Al occupying two-thirds of the octahedral (Na) interstices in an fcc oxide lattice. However, this structure is nonporous and does not readily form the hydroxide or absorb water.

The presence of the oxide thus does not appear to act as a barrier to oxidation close to the ignition point of the nanoparticles, but it can ''facilitate'' the oxidation reaction. Thus when the aluminum liquefies, at this point the nearest available oxygen atoms for oxidation come from the neighboring oxygen atoms in the aluminum oxide coating. As the aluminum oxidizes, heat is released, and as the coating loses oxygen, new oxygen atoms move into the aluminum from the outer surface.

As the temperature of the particles is further raised, the liquid aluminum gets ''contaminated'' with liquid aluminum oxide, hydroxide, nitrides, chlorides, etc. This occurs when the melting point, for example, for aluminum oxide of 2047°C, is reached. These impurities can be picked up during the ''healing'' oxidative process of the cracking oxide coating with the combustion gases such as chlorine, carbon monoxide, water, etc., produced by the burning propellant. The impurities further reduce the boiling point for aluminum. As they dissolve in the aluminum, surface oxidation of the droplet continues and accelerates. This is due to the fact that as the oxidation takes place, further heat is released, until the process accelerates to a point where the aluminum temperature has increased to the dissociation point of 2477°C, and the molten drop dissociates or ignites with a sudden flash.

Downloaded At: 13:46 16 January 2011

Discussion

High-resolution transmission electron microscopy has evidenced an oxide surface 2.5 nm in thickness with some crystalline layers possibly of α-alumina. The latter appear to exfoliate readily and allow water to permeate into the surface of the material, gradually transforming the alumina to the α-aluminum oxy-hydroxide form. The crystalline layers thus appear to have some mismatch, and the ready exfoliation of the surface crystalline layers explains the fast aging characteristics typical of the nanoaluminum particles. The incorporation of boron impurities in the α-forms of alumina can explain the marked black coloration of the nanoaluminum.

A small (1–2%) negative strain or compressive stress was detected in certain orientations of the nanoaluminum particles. The latter were related to the formation of the high-density α-alumina oxide on the surface of the nanoparticles, which transmits the natural compression of the surface aluminum oxide into the aluminum lattice that it surrounds or constrains. As the oxidation model shows, oxidation is favored when atomic space is allowed for the oxygen atoms to enter the aluminum interatomic lattice spaces. A compressive stress thus may not facilitate this process. Thus the initial presence of oxygen on the surface facilitates the oxidation, rather than forming a barrier, until there is no extra space for any additional oxygen adatoms to move into the lattice spacing after electric charge equilibrium has been reached. After this point is reached, the oxide can be considered as a barrier to further oxidation.

However, in the case of nanoaluminum, as a temperature of 500°C is approached, impurity catalyzed reactions have been detected to occur. These can produce gaseous molecules, which generate further interatomic space and more oxidation. In fact, the nanoaluminum particles are so small that with the aid of impurity-catalyzed reactions at $\sim$500°C oxygen can be allowed to permeate farther into the interior of the particle. Thus when the ignition point of $\sim$2000°C for aluminum is reached, some oxygen already may be present in the interior of the nanoparticle, which can trigger a heat release from inside, catalyzing a rapid inflammation. For a nanoparticle the oxygen incorporated per unit volume can be a lot. For the micron-sized aluminum in the liquid state one can consider that O_2 gets boiled off continuously, giving very high temperatures of inflammation.

That nanoparticles are likely to have a higher relative level or proportion of impurities is not only due to their small size but also to the extreme conditions of manufacturing under which they are made. Thus the very high temperatures required often involve the use of heat-resistant ceramic materials of various kinds, which come in contact with the base metal and from which the impurities may be picked up. The manufacturing process itself thus determines the species and level of impurities present in the nanoparticles.

Downloaded At: 13:46 16 January 2011

Table 3
Potential benefits of nanoaluminum distributed in propellant formulations compared with micron-sized aluminum

Nanoparticles of aluminum	Micron-sized aluminum particles
Surface agglomeration less likely	Surface agglomeration of micron-sized aluminum
Rapid inflammation Complete combustion	Longer time to reach inflammation point Incomplete combustion likely
Potential of more distributed homogeneous distribution	Less homogeneous distribution
Does not readily act as heat sink	Micron-sized particles take more time to heat and thus act as heat sink
Rapid transformation to ''semifluid'' state with corresponding fast ignition	In liquid state O_2 gets boiled off continuously, which increases temperature of inflammation
Weight impact of impurities is large, triggering autocatalyzed reactions, which increase rate of heat emission and facilitate oxygen incorporation	Impurities have little weight effect on micron-sized aluminum
Potential oxygen incorporated per unit volume can be large, triggering heat release and inflammation from inside	No large amount of oxygen incorporation possible
Potential of atomic-scale design for part-explosive nanoaluminum with, e.g., appropriate incorporation of nitrogen	Weight percent of incorporated impurities have little effect on micron-sized particles

Downloaded At: 13:46 16 January 2011

In fact, the nanoparticles can reach 2000°C more rapidly than the micron-sized particles and can be considered to reach a "semi-fluid" state quickly when heated, with a very rapid ignition. Furthermore the micron-sized aluminum can act as more of a heat sink in comparison to the nanosized aluminum, delaying the time for the overall temperature rise in a formulation. In addition, when one considers that nitrogen is one of the main constituent elements of explosives, the nitrogen present within the nanoaluminum potentially may be incorporated in such a way as to make the material "part-explosive" by triggering the appropriate physiochemical reaction. The incorporation of light-element-tailored impurities during the manufacture thus may provide for new improved forms of nanoaluminum by "atomic-scale design." Table 3 is a comparison between nanoaluminum and micron-sized aluminum, which summarizes some of the potential benefits of nanoaluminum compared with micron-sized aluminum, when the physiochemical phenomena occurring at the atomic or nanoscale are taken into account, for a more rapid burn in propellant formulations containing the same.

Downloaded At: 13:46 16 January 2011

Acknowledgments

The CAD/PAD Department, at NAVSEA-IH is thanked for the nanoaluminum samples and for support of some of the investigative work on nanoaluminum. Dr. Michael A. O'Keefe and Dr. Cheng Yu Song of the NCEM, Materials Science Division, Lawrence Berkley National Laboratory, are thanked for the high-voltage electron microscopy of clusters of nanoaluminum particles. Dr. Brad Forch is thanked for his valuable encouragement and guidance throughout. Dr. John Kolts and DTRA is thanked further for support under the Advanced Energetics Research Program FY02-WMR-044. Finally ARL is thanked for collaborative work on the project as a whole. The NCEM is supported by the Director, Office of Science, through the Office of Basic Energy Sciences, Material Sciences Division, of the U.S. Department of Energy, under contract No. DE-AC03-76SF00098. We express special gratitude to Dr. Richard Miller, retired, ONR.

References

[1] Price, E. W. 1984. Fundamentals of solid-propellant combustion. In K. Kuo and M. Summerfield (eds.), *Progress in Astronautics and Aeronautics*, American Institute of Aeronautics and Astronautics, New York, NY, vol. 90, p. 479.

[2] Zarko, V. E. 1998. Modelling and performance prediction in rockets and guns, In S. R. Chakravarthy and S. Krishnan (eds.), Allied Publishers, Chennai, India, p. 301.

[3] Hill, G. C. and J. S. Holman. 1978. *Chemistry in Context*. Nelson Publishers.

[4] Lide, D. R. *Handbook of Physics and Chemistry*. 2003. Boca Raton: CRC Press.

[5] Crump, J. E., J. L. Prentice, and K. J. Kraeutle. 1969. *Combustion Science and Technology*, 1: 205.

[6] Christensen, H. C., R. H. Knipe, and A. S. Gordon. 1965. *Pyrodynamics*, 3: 91.

[7] Marion, M., C. Chauveau, and I. Gokalp. 1996. *Combustion Science and Technology*, 115: 369–390.

[8] Ramaswamy, A. L., P. Kaste, and S. F. Trevino. 2005. *Journal of Energetic Materials*, 22: 1–24.

[9] Hooton, I. 2002. Nanopowders: Characterization studies, Proceedings of the DIA New Materials III Symposium, 2–4 April. The MITRE Corporation, McLean, Virginia.

[10] Palmer, D. 1998. *CrystalMaker*, Oxford: Holywell Press.

[11] Schaub, R., F. Wahlstrom, A. Ronnau, E. Laegsgaard, I. Stensgaard, and F. Besenbacher. 2003. *Science*, 299: 377.

[12] Thurmer, K., E. Williams, and J. Reutt-Robey. 2002. *Science*, 297: 2033.

[13] Finger, L. W. and R. M. Hazen. 1978. *Journal of Applied Physics*, 49: 5823.

[14] Megaw, H. D. 1973. *Crystal Structures: A Working Approach*, Philadelphia: W. B. Saunders, pp. 356–359.

[15] Greenwood, N. N. and A. Earnshaw. 1984. *Chemistry of the Elements*, New York: Pergamon Press, p. 277.

Downloaded At: 13:46 16 January 2011